European Journal of Pharmaceutical Sciences 189 (2023) 106557

Contents lists available at ScienceDirect

European Journal of Pharmaceutical Sciences

journal homepage: www.elsevier.com/locate/ejps

Freeze-dried nanocrystal dispersion of novel deuterated pyrazoloquinolinone ligand (DK-I-56-1): Process parameters and lyoprotectant selection through the stability study

Jelena R. Mitrović [a], Maja Bjelošević Žiberna [b], Aleksandar Vukadinović [c], Daniel E. Knutson [d], Dishary Sharmin [d], Aleksandar Kremenović [e], Pegi Ahlin Grabnar [b], Odon Planinšek [b], Dominique Lunter [f], James M. Cook [d], Miroslav M. Savić [g], Snežana D. Savić [a,*]

[a] Department of Pharmaceutical Technology and Cosmetology, University of Belgrade–Faculty of Pharmacy, Vojvode Stepe 450, Belgrade 11221, Serbia
[b] Department of Pharmaceutical Technology, University of Ljubljana, Faculty of Pharmacy, Aškerčeva 7, 1000, Ljubljana, Slovenia
[c] "VINČA" Institute of Nuclear Sciences – National Institute of the Republic of Serbia, University of Belgrade, Mike Petrovića Alasa 12-14, Belgrade, Serbia
[d] Department of Chemistry and Biochemistry, Milwaukee Institute for Drug Discovery, University of Wisconsin-Milwaukee, 3210N. Cramer St., Milwaukee, WI, United States
[e] Laboratory of Crystallography, Faculty of Mining and Geology, University of Belgrade, Đušina 7, Belgrade, Serbia
[f] Institute of Pharmaceutical Technology, Eberhard-Karls University, Auf der Morgenstelle 8, Tübingen, Germany
[g] Department of Pharmacology, University of Belgrade – Faculty of Pharmacy, Vojvode Stepe 450, Belgrade, Serbia

ARTICLE INFO

Keywords:
Pyrazoloquinolinone
Nanocrystals
Freeze-drying
Sucrose
Trehalose
Mannitol

ABSTRACT

Recently, nanocrystal dispersions have been considered as a promising formulation strategy to improve the bioavailability of the deuterated pyrazoloquinolinone ligand DK-I-56-1 (7-methoxy-2-(4-methoxy-d3-phenyl)-2,5-dihydro-3H-pyrazolo[4,3-c]quinolin-3-one). In the current study, the freeze-drying process (formulation and process parameters) was investigated to improve the storage stability of the previously developed formulation. Different combinations of lyoprotectant (sucrose or trehalose) and bulking agent (mannitol) were varied while formulations were freeze-dried under two conditions (primary drying at -10 or -45 °C). The obtained lyophilizates were characterized in terms of particle size, solid state properties and morphology, while the interactions within the samples were analyzed by Fourier transform infrared spectroscopy. In the preliminary study, three formulations were selected based on the high redispersibility index values (around 95%). The temperature of primary drying had no significant effect on particle size, but stability during storage was impaired for samples dried at -10 °C. Samples dried at lower temperature were more homogeneous and remained stable for three months. It was found that the optimal ratio of sucrose or trehalose to mannitol was 3:2 at a total concentration of 10% to achieve the best stability (particle size < 1.0 μm, polydispersity index < 0.250). The amorphous state of lyoprotectants probably provided a high degree of interaction with nanocrystals, while the crystalline mannitol provided an elegant cake structure. Sucrose was superior to trehalose in maintaining particle size during freeze-drying, while trehalose was more effective in keeping particle size within limits during storage. In conclusion, results demonstrated that the appropriate combination of sucrose/trehalose and mannitol together with the appropriate selection of lyophilization process parameters could yield nanocrystals with satisfactory stability.

1. Introduction

Several pyrazoloquinolinone compounds synthesized in the 1980s were found to be the first non-benzodiazepine ligands to selectively bind to the benzodiazepine site on $GABA_A$ receptors. More recently, a series of analogs with functional selectivity for $GABA_A$ receptors containing the α6 subunit have been prepared by targeted structural modifications. The distribution and role of these receptors make the newly synthesized pyrazoloquinolinones potentially useful not only for the treatment of various neuropsychiatric disorders such as essential tremor, tic disorders, trigeminal pain, and migraine (Sieghart et al., 2022), but also for preventing the ataxic effects of benzodiazepines without interfering

* Corresponding author.
E-mail address: snezana.savic@pharmacy.bg.ac.rs (S.D. Savić).

https://doi.org/10.1016/j.ejps.2023.106557
Received 15 May 2023; Received in revised form 2 August 2023; Accepted 3 August 2023
Available online 6 August 2023

with their other psychomotor or anticonvulsant effects (Divović Matović et al., 2022). To increase metabolic stability and bioavailability, deuterated analogues, including DK-I-56-1 (7-methoxy-2-(4-methoxy-d3-phenyl)-2,5-dihydro-3H-pyrazolo[4,3-c]quinolin-3-one), have been developed. Deuteration of a methoxy group increased the stability of DK-I-56-1 to O-demethylation, as well as bioavailability and brain exposure. Among all synthesized deuterated derivatives, DK-I-56-1 was selected as the lead ligand for future studies based on its good pharmacological profile and relative ease of synthesis (Knutson et al., 2018).

Due to low solubility of DK-I-56-1 in water as well as in many commonly used oils, co-solvents, and organic solvents, nanocrystal dispersion has been chosen as a formulation strategy to further improve bioavailability and enable future drug development (Mitrović et al., 2020). Nanocrystal dispersions are submicron size dispersions of drug nanoparticles stabilized by surfactants, polymers, or their combination (Al-Kassas et al., 2017). Due to their small particle size, low concentration of stabilizers, and absence of organic solvents, they are considered biocompatible formulations that have been studied for almost all routes of administration (Patel et al., 2020). In our recent article, parenteral nanocrystal dispersions of DK-I-56-1 were developed and prepared by small-scale wet ball milling technique. The selected formulations exhibited small and uniform particle size with acceptable short-term stability (three weeks), retained crystalline structure of DK-I-56-1, and improved bioavailability after intraperitoneal administration. *In vivo* pharmacokinetic and pharmacodynamic studies confirmed their suitability as a promising platform for preclinical development (Mitrović et al., 2020).

However, the small particle size of nanocrystals makes them susceptible to aggregation during storage, which is considered the major drawback of these systems (Wu et al., 2011; Li et al., 2021). For parenteral formulations, it is important to keep the particle size below 1 μm; therefore, to extend shelf life, nanocrystal dispersions are usually solidified by freeze-drying or spray-drying. Freeze-drying is widely used as a drying method for various nanoparticle formulations, including nanocrystals (Jakubowska et al., 2022; Trenkenschuh and Friess, 2021). However, the process itself could have negative effects on particle size. During freezing, the nanocrystals are separated from the ice crystals into the nanoconcentrated phase, where there is a high probability of aggregation due to the reduced spacing between particles (Yue et al., 2014). The addition of cryoprotectants prevents aggregation thanks to the minimized mobility of nanoparticles in the highly viscous glassy matrix (Mohammady et al., 2020; Niu and Panyam, 2017). The mechanism explained is the basic principle of vitrification theory when the freezing temperature is kept below the glass transition temperature of the maximum freeze-concentrated solution (Tg') (Abdelwahed et al., 2006a). During primary drying, sublimation of water leads to the disintegration of the stabilizer layer of the nanoparticles, resulting in aggregation of the particles. Lyoprotectants stabilize nanoparticles by replacing the hydrogen bonds of water, as explained by the water replacement hypothesis (Trenkenschuh and Friess, 2021).

Disaccharides are the most commonly used cryoprotectants/lyoprotectants, including sucrose and trehalose in particular. In addition to their stabilizing effect, these substances also act as tonicity agents, increase product mass, and facilitate rehydration of freeze-dried cakes (Bjelošević et al., 2020). The quality of freeze-dried products depends on the process and formulation parameters, including the choice of cryo/lyoprotectant and its concentration (Jakubowska et al., 2022; Beirowski et al., 2011). Furthermore, bulking agents can be added to increase mechanical strength and ensure an attractive appearance of the cake. Mannitol, which crystallizes readily upon freezing, is most commonly used as a bulking agent (Trenkenschuh and Friess, 2021). Although the combination of the cryoprotectant/lyoprotectant and the bulking agent is common in biopharmaceutical products, this approach is not widely used in freeze-drying nanocrystal dispersions. Since sucrose and trehalose are usually used simultaneously as cryoprotectants and lyoprotectants, they will be referred to as lyoprotectants in the remainder of the manuscript.

The focus of this research was to establish process and formulation parameters in freeze-drying of DK-I-56-1 nanocrystal dispersion to obtain lyophilizates with enhanced stability. First, the stability of nanocrystals during freeze-drying was studied in the presence of sucrose or mannitol alone or in different combinations to select their appropriate concentrations. Two freeze-drying procedures were used with different primary drying temperatures: -10 or -45 °C, above or below the Tg' values previously determined by differential scanning calorimetry. Selected formulations containing sucrose or trehalose as lyoprotectant in combination with mannitol as bulking agent were characterized physicochemically and stored for three months. The stability of the freeze-dried samples was evaluated by measuring particle size and calculating redispersibility index, as well as by solid-state analysis (by differential scanning calorimetry and X-ray powder diffraction) and visualization of morphology (by scanning electron microscopy and polarized light microscopy). Finally, the extent of interactions between the nanocrystal stabilizers and the lyoprotectant was evaluated by Fourier transform infrared spectroscopy (FT-IR).

2. Material and methods

2.1. Material

DK-I-56-1 was synthesized at the University of Wisconsin—Milwaukee, USA according to the protocol given in Knutson et al. (2018). Other substances used in the research were as followed: polysorbate 80, mannitol, sucrose (Sigma-Aldrich Laborchemikalien GmbH, Germany), and poloxamer 407 (BASF Ludwigshafen, Germany) and trehalose dihydrate (Carl Roth GmbH, Germany). Fresh ultrapure water used for reconstitution was supplied from a TKA GenPure system (TKA Wasseranfbereitungssysteme GmbH, Germany).

2.2. Nanocrystal dispersion preparation

The nanocrystal dispersion of DK-I-56-1 was prepared according to the same protocol described in Mitrović et al. (2020). Briefly, DK-I-56-1 was dispersed in a solution of polysorbate 80 and poloxamer 407 (the ratio between polysorbate 80 and poloxamer 407 was 1:1) and mixed on a rotor-stator homogenizer IKA Ultra-Turrax® T25 digital (IKAR-Werke GmbH & Company KG) at 10 000 rpm for 5 min. The obtained dispersion was transferred to 2 ml Eppendorf tubes containing 60% v/v 0.1-0.2 mm yttrium-stabilized zirconium beads (SiLibeads® type ZY-S, Sigmund Lindner, Germany). To reduce the particle size, the tubes were shaken for 1 h with a bead grinding cell disruptor (Disruptor Genie, Scientific Industries, USA) with the maximum speed set at 2850 rpm. Afterwards, the nanocrystal dispersion was separated from the beads and stored in a glass bottle. The concentration of DK-I-56–1 was 2.0 mg/ml, while the total concentration of stabilizers was 1.0 mg/ml.

Prior lyophilization, lyoprotectants and bulking agent were added to 2 ml of nanocrystal dispersion. In the first lyophilization (marked as lyophilization-1) following pharmaceutical excipients were added: mannitol 5% (M 5%), mannitol 10% (M 10%), sucrose 10% (S 10%), sucrose and mannitol in ratio 2:1 in total concentration 10% (S+M 2 + 1 10%), sucrose and mannitol in ratio 3:2 in total concentration 10% (S+M 3 + 2 10%), sucrose and mannitol in ratio 1:1 in total concentration 10% (S+M 1 + 1 10%), sucrose and mannitol in ratio 2:1 in total concentration 6% (S+M 2 + 1 6%). In second lyophilization (lyophilization-2) following excipients were added in total concentration 10%: sucrose (S), sucrose and mannitol in ratio 1:1 (S+M 1 + 1), sucrose and mannitol in ratio 3:2 (S+M 3 + 2), trehalose (T), trehalose and mannitol in ratio 1:1 (T+M 1 + 1), trehalose and mannitol in ratio 3:2 (T+M 3 + 2).

2.3. Lyophilization

Lyophilization was performed under two conditions. For lyophilization-1, samples were frozen at -80 °C for 3 h and then freeze-dried in a Beta 1–8 K freeze dryer (Martin Christ, Osterode am Harz, Germany) for 24 h, with primary drying at -10 °C and 0.340 mbar and secondary drying at 25 °C. Samples were stored in sealed vials at 25 °C, and physicochemical characterization was performed immediately after freeze-drying and after one month of storage. For lyophilization-2, samples were frozen at -50 °C for 3 h and then primary dried at -45 °C and 0.2 mbar for 21 h, which was followed by secondary drying at 20 °C for 30 h in a Telstar LyoBeta Mini freeze dryer (Spain). Vials were vacuum sealed, crimped, and stored in the refrigerator (2-8 °C) for three months. After lyophilization all cakes were inspected visually and photographed. The classification of the products based on the cake appearance was made according to the terminology used in the article by Patel et al. (2017). Characterization was performed immediately after freeze-drying and after one and three months of storage.

2.4. Particle size analysis

Particle size (mean hydrodynamic radius, z-ave) and particle size distribution (polydispersity index, PDI) were measured by dynamic light scattering using the Zetasizer Nano ZS90 (Malvern Instruments Ltd., Worcestershire, UK). These parameters were determined in samples before lyophilization (z-ave$_{\text{before lyo}}$) and in freeze-dried samples after reconstitution (z-ave$_{\text{after lyo}}$). Freeze-dried formulations were dispersed in ultrapure water to achieve the same concentration of DK-I-56-1 as in the dispersion before lyophilization, by manual shaking for maximum 30 s. Before measurement, the nanocrystal dispersions were diluted in ultrapure water (1:100, v/v). Reconstitution and particle size measurement were performed right after freeze-drying, and one and three months after freeze-drying. The redispersibility index (RDI) was calculated using the following equation:

$$RDI(\%) = \frac{z - ave_{before\ lyo}}{z - ave_{after\ lyo}} \times 100$$

To detect particles larger than 1 μm, laser diffraction (LD) was used as an additional particle measurement method after one month of storage. Measurements were performed using a Mastersizer (Malvern Mastersizer 2000 equipped with a small volume dispersion cell, Malvern, UK). Results are reported as d(0.1), d(0.5), and d(0.9), representing 10%, 50%, and 90% of the particle volume below a certain size, respectively, and D[4,3] as the volume-weighted mean diameter.

All particle size measurements were done in triplicates. Results are expressed as mean ± standard deviation. Statistical analysis included Student t-test (for two sets of results) or one-way ANOVA (for three sets of results) with Tukey HSD as a post hoc test. P values < 0.05 were considered as statistically significant. Statistical analysis was done using IBM SPSS Statistics software (v.25).

2.5. Differential scanning calorimetry (DSC)

To determine the glass transition temperature of the maximally freeze-concentrated solution (Tg'), liquid samples were cooled from 25 °C to -80 °C at a rate of -0.5 °C/min and then heated to 50 °C at a rate of 10 °C/min. The value of Tg' was characterized as the midpoint of the glass transition. This analysis was performed for the nanocrystal dispersions with lyoprotectants and for aqueous solutions of lyoprotectants in the same concentration (labeled as placebo). To characterize the final lyophilizates, samples were cooled from 25 °C to -30 °C (cooling rate 10 °C/min), held at -30 °C for one minute, and then heated to 230 °C at a rate of 10 °C/min. All measurements were performed using DSC1 (Mettler Toledo, Switzerland) under a nitrogen flow of 50 ml/min. The thermoanalytical parameters were calculated using STAR® software SW 12.10.

2.6. X-ray powder diffraction (XRPD)

The physical state of the freeze-dried samples was analyzed by X-ray powder diffraction (XRPD). The analysis was performed on a Rigaku Smartlab X-ray diffractometer in a θ-θ geometry using the D/teX Ultra 250 strip detector in 1D standard mode with a CuK$\alpha_{1,2}$ radiation source (U=40 kV and I=30 mA). Data were acquired in a 2θ range of 3-40° using a low background single crystal silicon sample holder to minimize background. Results were analyzed using PDXL2 (v. 2.8.30) integrated X-ray powder diffraction software.

2.7. Scanning electron microscopy (SEM)

The morphology of the lyophilzates was analyzed by scanning electron microscopy (SEM). A small amount of the sample was placed on a conductive double-sided adhesive tape and examined with a Zeiss Ultra Plus 55 or Zeiss DSM 940 A microscope (Carl Zeiss GmbH, Oberkochen, Germany). Photomicrographs were taken at different magnifications (5000 or 20,000 ×), and the exact magnification for each sample is indicated in the caption as well as in the bar size.

2.8. Polarized light microscopy (PLM)

Physical state and morphology of the freeze-dried samples were also analyzed using polarized light microscopy (PLM). It was performed using Carl Zeiss ApoTome Imager Z1 microscope (Zeiss, Germany) with crossed polarizers and ¼ λ-plate. Photomicrographs were taken under 400 × magnification with the digital camera and processed with the appropriate software.

2.9. Fourier transform infrared (FT-IR) spectroscopy

The interactions between lyoprotectants and nanocrystal stabilizers were analyzed by Fourier transform infrared spectroscopy (FT-IR). The analysis was performed using a Nicolet iS10 (Thermo Scientific, Waltham, MA, USA) FT-IR spectrometer equipped with a single reflection ATR system (Smart iTR, Thermo Scientific, USA) with diamond plate and ZnSe lens. Spectra were recorded in the range of 4000 cm^{-1} to 660 cm^{-1} with a resolution of 0.5 cm^{-1}.

3. Results and discussion

3.1. Preliminary study

3.1.1. Lyoprotectant screening

Several factors can affect the redispersibility of freeze-dried nanocrystals. To prevent aggregation of nanoparticles during freeze-drying, lyoprotectants are added at different concentrations. The type and concentration of these excipients have been shown to have a strong influence on redispersibility (Jakubowska et al., 2022), so screening of lyoprotectants was the first step of the preliminary study. The formulation of interest in this research is intended for parenteral administration, so these additives can be used simultaneously as tonicity agents, since nanocrystals as undissolved particles would not contribute significantly to the tonicity of the formulation. Therefore, the concentration of lyoprotectants and bulking agent was initially adjusted to achieve the isotonic formulation. Nanosuspensions were freeze-dried by the lyophilization-1 and the results of particle size analysis after redispersion are shown in Fig. 1. Mannitol did not prevent aggregation (RDI around 60%) at either concentration (5% and 10%), which was expected despite its frequent use in nanocrystal lyophilization. Mannitol could be considered a bulking agent rather than a cryoprotectant, so its stabilizing effect was not pronounced (Trenkenschuh and Friess, 2021).

In contrast, when sucrose alone was used (S 10%), aggregation did not occur, PDI was not significantly altered, and RDI was around 95%. Sugars, such as sucrose, are the lyoprotectants of choice for many

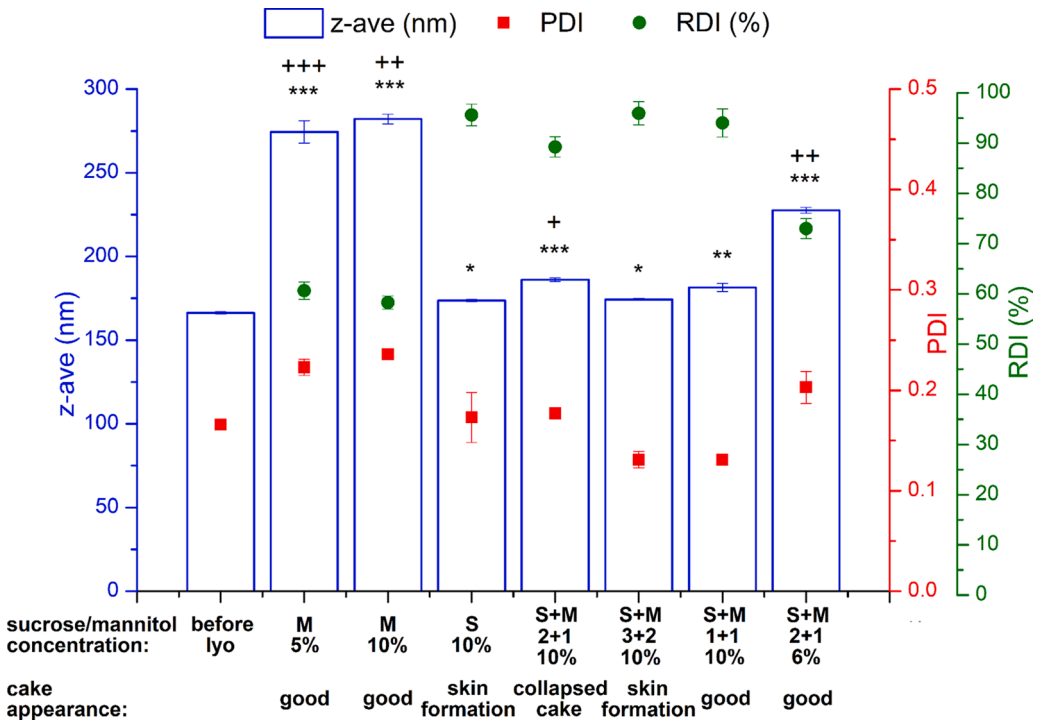

Fig. 1. Mean hydrodynamic diameter (z-ave), polydispersity index (PDI) and redispersibiliy index (RDI) after lyophilization of nanocrystal dispersion with different sucrose/mannitol ratios (z-ave: *, ** and *** for $P < 0.05$, 0.01 and 0.001, respectively, PDI: +, ++ and +++ for $P < 0.05$, 0.01 and 0.001, respectively), Description of the cake appearance was based on the terminology given in Patel et al. (2017).

nanoparticle formulations. The flexible structure of disaccharides contributes to their stabilization mechanisms of vitrification/particle isolation and water replacement (Yue et al., 2013, 2014). The concentration of 10% was also found to be suitable for stabilization of various nanoparticle formulations (Trenkenschuh et al., 2021). Regarding the appearance of the cake, the observed ''skin formation'', a relatively dense layer of solid on the surface of the cake does not necessarily indicate insufficient quality if other parameters are unchanged (in this case, if no aggregation occurred). It is possible that the observed structure was formed during phase separation in the freezing step and does not affect the dynamics of the drying phase (Patel et al., 2017).

As mentioned above, mannitol is rarely used as a cryoprotectant because of its high crystallization tendency. It is more commonly used as a bulking agent that provides mechanical support to the cake (Trenkenschuh and Friess, 2021). Therefore, we investigated the addition of mannitol at different concentrations and its effects on stability. No aggregation occurred when using different combinations of sucrose and mannitol at a total concentration of 10% (S+M 2 + 1 10%, S+M 3 + 2 10%, and S+M 1 + 1 10%). The particle size remained almost the same and the PDI was less than 0.200, indicating uniform particle size. However, at a sucrose to mannitol ratio of 2 to 1 (S+M 2 + 1 10%), the cake collapsed, which was a reason to exclude this formulation from further studies. In this case, it was possible that at a lower mannitol concentration in sucrose-mannitol mixtures, the mannitol did not crystallize completely during the freezing step. To prevent the observed collapse, an additional annealing step in the freeze-drying process is usually recommended (Johnson et al., 2002).

After reconstitution, the osmolality of the formulations S 10%, S+M 1 + 1 10% and S+M 3 + 2 10% was tested. The values obtained were 345, 495, and 475 mOsm/kg, respectively, for the above formulations, making them hypertonic preparations. To obtain an isotonic formulation, the total concentration of sucrose and mannitol was reduced to 6% (S+M 2 + 1 6%). In this formulation, although the appearance of the cake was good, the particle size and PDI were significantly increased, while the RDI had decreased to below 80%, indicating insufficient sucrose concentration. This was considered unacceptable and this combination was excluded from further testing. Although isotonic preparations are preferable, hypertonic formulations are acceptable for parenteral administration, especially if the stability of such formulations depends on the excipients that contribute to their tonicity (Wang, 2015). Therefore, based on the observations in the screening phase, three samples were selected for the stability study: S 10%, S+M 1 + 1 10%, and S+M 3 + 2 10%.

3.1.2. Determination of the glass transition temperature of the maximally freeze-concentrated solution (Tg')

The glass transition temperature of the maximally freeze-concentrated solution (Tg') was determined by differential scanning calorimetry (DSC). This parameter was evaluated in aqueous solutions of lyoprotectants and bulking agent at the same concentration as in the nanocrystal formulations (placebo samples) and in the samples prepared for freeze-drying (nanocrystal dispersion). The Tg' values of the samples with sucrose only presented in Table S1 agreed well with the values found in the literature (Meng-Lund et al., 2019). The thermal event that could be characterized as the eutectic temperature was not detected in either sample containing mannitol. The obtained Tg' values did not substantially differ between placebo and nanocrystal dispersions. Although in some cases the addition of nanocrystals could lead to slight changes in Tg' (Gol et al., 2018), the obtained differences are not considered significant. Nanocrystal particles should be present in the cryo-concentrated phase during freezing (Yue et al., 2014), but they would remain dispersed as crystal structures, detached from the frozen solution of cryoprotectants. In this way, the Tg' parameter would depend solely on the cryoprotectants (Holzer et al., 2009).

During freezing, as the temperature is lowered, phase separation occurs with the formation of two regions within the sample - ice crystals and cryo-concentrated (or nano-concentrated) phase. In the latter phase, the distance between nanoparticles decreases, increasing the probability of aggregation. In the presence of cryoprotectants, at a temperature below Tg', this phase transforms into a glassy state in which the particles

are immobilized. Therefore, for effective cryopreservation, a freezing temperature below Tg' should be achieved (Abdelwahed et al., 2006b; Yue et al., 2014), and this condition was met in both freeze-drying processes, while the freezing rate could be considered similar. The conditions for primary drying also depend on this parameter. In this lyophilization phase, the temperature of the formulation should be kept below the critical formulation temperature (CFT). At this temperature, the internal morphology of the product begins to change, resulting in significant changes in the specific surface area of the cake structure or loss of structure. It has been found that this parameter is usually about 2-5 °C higher than the corresponding Tg'. However, it has been shown that the formulation design is also an important factor for stability, especially when steric hindrance is provided by stabilizers (Beirowski et al., 2011).

Furthermore, the addition of bulking agent allows primary drying above Tg' or CFT. Above this temperature, the amorphous material is not rigid enough to support its own weight, so mechanical support from the crystalline component prevents macroscopic collapse (L Remmele et al., 2012). In our study, despite the high temperature during primary drying (-10 °C), we did not observe any collapse of the cake in the sample with sucrose only. For excipients such as mannitol, which are prone to crystallization, primary drying can be performed at temperatures just below their eutectic point (-1.5 °C), so the combination of sucrose and mannitol has the advantages of both systems. With a sufficient amount of mannitol (at least 30%), the cake structure is secured by its crystallinity even if primary drying is carried out at -10 °C, while amorphous sucrose could provide stabilization of the nanocrystals (Johnson et al., 2002). The cake collapse observed in the S+M 2 + 1 10% sample is consistent with these statements. In this sample, the mannitol was probably not completely crystalline due to its low concentration (Kim et al., 1998).

3.2. Particle size analysis and stability study

In the present study, two freeze-drying processes were compared, with primary drying above or below Tg' (-10 °C in lyophilization-1 and -45 °C in lyophilization-2, respectively), in terms of particle size preservation during the drying process and stability during storage. Based on the results from the screening phase, three formulations were selected for the stability study. The results of particle size after freeze-drying at -10 °C (lyophilization-1) are shown in Table 1 and images of formulation are given in Figure S1. After freeze-drying, the particle size remained more or less unchanged, with a slight increase in particle size of about 10 nm and an unchanged PDI, while the RDI was above 94% for all three formulations. These findings confirmed the results of the screening phase.

The freeze-dried samples were stored in sealed vials at 25 ± 2 °C for one month. After reconstitution, particle size increased dramatically in all formulations ($P < 0.001$), despite good redispersibility immediately after lyophilization. The size of the particles doubled, decreasing the RDI to about 50% or less, with high PDI values indicating a broad particle size distribution. Massive agglomeration was confirmed by LD, where particles larger than 1 μm were detected (Table S2). It appears that the instability observed in this part of the research was a kinetic rather than a thermodynamic process and was likely caused by the close interaction of the nanoparticles, which has led to irreversible aggregation. This could be the consequence of vitrification of the steric stabilizers or the inadequate structure of the cake. The aggregation that occurred during storage could be caused by the change from the glassy to the rubbery state of the steric stabilizers (polysorbate 80 and/or poloxamer 407). In this case, the nanoparticles would become mobile and could form solid aggregates. This process is favored at higher storage temperatures and in the presence of high moisture content (Yue et al., 2016).

Interestingly, sucrose alone was not effective as a stabilizer when primary drying was performed at -45 °C (Table 2). The agglomeration of nanocrystals was reflected in an increase in particle size of more than 100 nm and a PDI exceeding 0.300. The population of particles larger than 1 μm was detected by LD after one month of storage, confirming the DLS results (Table S3). After the additional month of storage, the cake collapsed (Figure S2), indicating an unstable structure of the lyophilizate. Therefore, the addition of mannitol was confirmed as necessary. In formulations with sucrose and mannitol in a 1:1 ratio (S+M 1 + 1), the particle size has significantly increased by about 30 nm during lyophilization ($P < 0.01$), reducing the RDI to about 80%. On the other hand, in formulation with sucrose and mannitol in a 3:2 ratio (S+M 3 + 2), the particle size remained almost unchanged (P=0.089). The PDI did not change significantly in either formulation ($P > 0.05$). It remained below 0.200, indicating that massive agglomeration did not occur despite the increase in particle size observed in S+M 1 + 1. In these formulations, the particle size remained in the nanometer range after freeze-drying, which was confirmed by the LD results after one month of storage

Table 1
Mean hydrodynamic diameter (z-ave), polydispersity index (PDI), redispersibiliy index (RDI) and cake appearance of nanocrystal dispersions before lyophilization-1, and following reconstitution right after lyophilization and after one month of storage at 25 °C.

Formulation	z-ave (nm)	PDI	RDI (%)	Cake appearance*
before lyophilization S 10%	166.1 ± 3.2	0.123 ± 0.018	-	-
after lyophilization	173.7 ± 0.7	0.173 ± 0.025	95.61 ± 2.15	skin formation
one month	485.1 ± 27.3	0.483 ± 0.036	34.28 ± 1.24	skin formation
S+M 1 + 1 10%				
after lyophilization	176.7 ± 2.0	0.135 ± 0.015	94.04 ± 2.81	acceptable
one month	299.7 ± 2.1	0.258 ± 0.002	55.43 ± 0.77	acceptable
S+M 3 + 2 10%				
after lyophilization	173.1 ± 0.9	0.143 ± 0.016	95.95 ± 2.31	skin formation
one month	353.3 ± 7.0	0.350 ± 0.013	47.02 ± 0.84	skin formation

* Description based on the terminology given in Patel et al. (2017).

Table 2
Mean hydrodynamic diameter (z-ave), polydispersity index (PDI), redispersibiliy index (RDI) and cake appearance of nanocrystal dispersions before lyophilization-2 with sucrose as a lyoprotectant, and following reconstitution right after lyophilization and after one and three months of storage at 2-8 °C.

Formulation	z-ave (nm)	PDI	RI (%)	Appearance
before lyophilization S	181.5 ± 3.2	0.174 ± 0.005	-	-
after lyophilization	355.8 ± 9.7	0.389 ± 0.063	51.02 ± 1.56	acceptable
one month	295.1 ± 2.1	0.332 ± 0.045	61.50 ± 1.46	partial collapse
three months	n.d.	n.d.	n.d.	collapsed cake
S+M 1 + 1				
after lyophilization	216.6 ± 3.3	0.117 ± 0.012	83.78 ± 0.30	acceptable
one month	213.8 ± 2.7	0.167 ± 0.023	84.97 ± 2.36	acceptable
three months	227.3 ± 7.0	0.098 ± 0.044	79.89 ± 3.06	acceptable
S+M 3 + 2				
after lyophilization	188.0 ± 2.0	0.132 ± 0.035	96.54 ± 1.15	acceptable
one month	189.8 ± 2.6	0.147 ± 0.020	95.65 ± 2.87	acceptable
three months	191.3 ± 3.4	0.165 ± 0.018	94.88 ± 3.01	acceptable

*Description based on the terminology given in Patel et al. (2017).

(Table S3). During three months of storage, the particle size and PDI were not further significantly changed (Table 2).

In lyophilization-2, trehalose was used in the same manner as sucrose. The results of particle size measurements are shown in Table 3 and images of obtained cakes could be seen in Figure S2. Particle size in formulations with trehalose increased to a greater extent during lyophilization, especially in formulations with trehalose alone and trehalose and mannitol in a 1:1 ratio ($P < 0.001$), although the PDI was not significantly changed. The differences between the samples with sucrose and trehalose could be explained by a different phase separation during lyophilization in the presence of these excipients. In a study with proteins, sucrose was more efficient than trehalose during the primary drying phase. It was shown that trehalose-rich regions induced larger areas where lysozyme had no protection against ice and ice sublimation (Starciuc et al., 2020). The same reasoning could be applied in this study. After three months of storage, particle size was not significantly increased (P=0.997 and 0.951 for T+M 1 + 1, after one and three months, respectively; $P = 0.260$ and 0.937 for T+M 3 + 2, after one and three months, respectively), except for the formulation with trehalose alone, for which an additional increase of approximately 20 nm was observed after three months of storage ($P < 0.05$). LD results after one month of storage were in line with DLS results (Table S3). Therefore, despite the initial increase in particle size, the nanocrystals remained in the nanometer range with a relatively narrow size distribution during storage.

To facilitate comparison of particle size in different formulations, the redispersibility index was calculated (RDI). This parameter allows a better understanding of the changes in particle size, as it reflects the relative particle size change during the observed period. After lyophilization-1, an RDI of about 95% was obtained in all formulations, but it dropped to values of 30-50% after only one month of storage. This was characterized as a loss of nanocrystalline structure. The highest RDI value in lyophilization-2 was achieved when sucrose and mannitol were used in a 3:2 ratio; it remained at about 95% throughout the storage period. In the formulation with trehalose, the highest redispersibility index was reached for the same ratio (3:2), although it was below 90%. This indicated that the mentioned ratio might be the best option for particle size maintenance.

Table 3
Mean hydrodynamic diameter (z-ave), polydispersity index (PDI), redispersibiliy index (RDI) and cake appearance of nanocrystal dispersions before lyophilization-2 with trehalose as a lyoprotectant, and following reconstitution right after lyophilization and after one and three months of storage at 2-8 °C.

Formulation	z-ave (nm)	PDI	RI (%)	Appearance
before lyophilization	205.5 ± 4.6	0.161 ± 0.051	-	-
T				
after lyophilization	289.9 ± 2.7	0.150 ± 0.017	73.43 ± 1.79	broken cake
one month	286.8 ± 4.8	0.140 ± 0.020	71.66 ± 0.74	broken cake
three months	299.6 ± 5.7	0.186 ± 0.032	68.60 ± 2.22	acceptable
T+M 1 + 1				
after lyophilization	279.9 ± 1.6	0.155 ± 0.045	73.41 ± 1.42	acceptable
one month	280.7 ± 2.6	0.155 ± 0.017	73.21 ± 1.02	acceptable
three months	278.7 ± 7.4	0.153 ± 0.038	73.78 ± 3.14	acceptable
T+M 3 + 2				
after lyophilization	227.9 ± 1.3	0.176 ± 0.021	90.18 ± 1.60	acceptable
one month	236.1 ± 5.8	0.180 ± 0.006	87.11 ± 3.87	acceptable
three months	238.4 ± 6.6	0.186 ± 0.023	86.26 ± 3.82	acceptable

*Description based on the terminology given in Patel et al. (2017).

For samples lyophilized by the process with primary drying at -45 °C, the RDI values obtained were generally lower but constant over a longer period of time. This suggested that changes had occurred during the freeze-drying process, while the rigid structure of the cakes prevented instability problems during storage. An exception was the sample with sucrose only, which collapsed with the loss of structure. The observed collapse impaired the quality of the freeze-dried sample. Redispersibility is the most important parameter that indicates the stability during storage, and drug nanocrystals are usually considered very stable if their redispersibility does not change significantly during storage (Beirowski et al., 2011). Since parenteral formulations are in focus, the dispersions should be redispersed rapidly and maintain nanometer particle size. All formulations obtained by lyophilization-2, with the exception of sample S, meet these requirements and extend shelf-life more than threefold compared to the liquid state formulation published in Mitrović et al. (2020).

3.3. Physical state analysis

Analysis of the physical state of the freeze-dried formulations included differential scanning calorimetry (DSC) and X-ray powder diffraction (XRPD). The evaluation of the physical state of the excipients was the main focus of this part of the research. DK-I-56-1 has a high melting point (312 °C), which is higher than the degradation point of sugars. Together with the low concentration of DK-I-56-1, this was the reason why the physical state of DK-I-56-1 could not be analyzed by DSC. In addition, DK-I-56-1 could not be detected by XRPD due to its low concentration and low intensity of diffraction peaks when it is in nanocrystalline form. The crystal structure of DK-I-56-1 in nanocrystalline formulation was confirmed in Mitrović et al. (2020), and would probably not change during lyophilization.

The main disadvantage of the lyophilization at higher temperatures is the possibility of formation of unstable mannitol hemihydrate (Johnson et al., 2002). The occurrence of this form of mannitol in the S+M 1 + 1 10% sample was evidenced by the characteristic DSC pattern of dehydration and subsequent crystallization at temperatures around 80 °C (Fig. S3), similar as in Anko et al. (2019) and Liao et al. (2007). Based on the DSC data and taking into account the observed glass transition and low enthalpy of fusion, this sample was considered as partially crystalline. However, the glass transition temperature was very low, so the stability of the cake during storage at 25 °C was probably compromised. After one month of storage, the cake was completely crystalline, as proven by the XRPD data, in which only the δ-form of mannitol was detected (data not shown). Small amounts of lattice water, which may have been released during the conversion of mannitol hemihydrate, may have had a plasticizing effect and negatively affected the stability of the product (Liao et al., 2007). The formulation containing sucrose and mannitol in a 3:2 ratio was completely crystalline immediately after lyophilization, with dominantly δ-form of mannitol present in the cake (Fig. S3) and remained in this state during storage (data not shown).

In the formulations with sucrose obtained by lyophilization-2, the crystallinity of sucrose was different when used alone or in various combinations with mannitol (Fig. 2). As can be seen from the very sharp melting peak and the well-defined diffraction signals, sucrose was in a crystalline state when used alone. This was unexpected since the temperature during freezing and primary drying was below Tg' (-32 °C). However, it was possible that despite the controlled shelf temperature of -45 °C, the sample temperature was actually around Tg'. Another possible explanation could lie in the formulation itself. The crystalline structure of the nanocrystals could have promoted the crystallization of sucrose. Despite the crystalline structure of the sample, the cake shrank and collapsed during storage. According to the XRPD measurements, the position and width of the signals changed in a sample stored for three months, indicating a reduction of the unit cell as well as the dimensions of the sucrose crystallites by about 20% (data not shown).

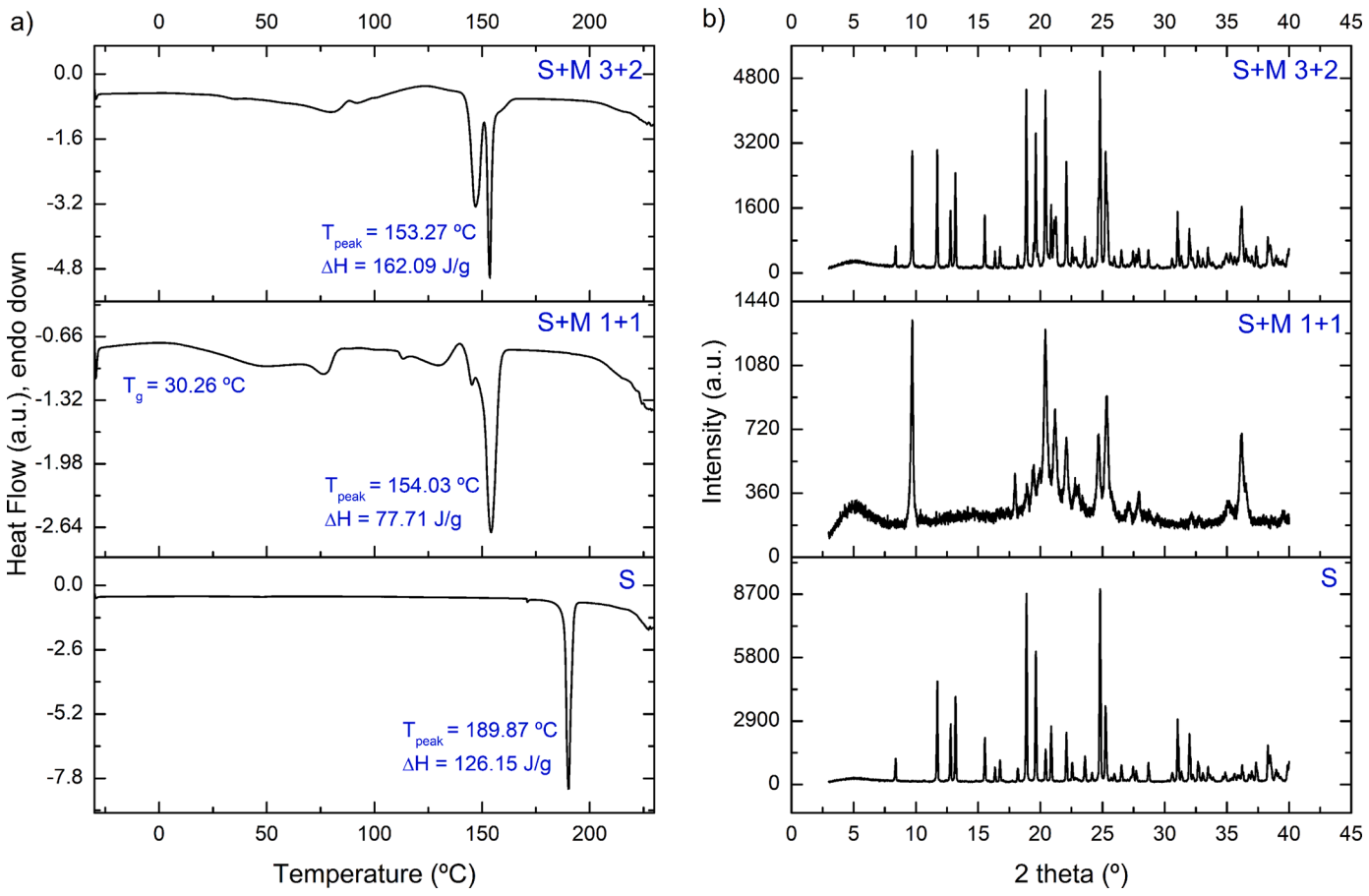

Fig. 2. DSC thermograms (a) and XRPD diffractograms (b) of freeze-dried samples with sucrose as cryo-/lyoprotectant obtained by lyophilization-2.

When mannitol was added in equal amount as sucrose (S+M 1 + 1), sucrose was amorphous, as indicated by the diffuse XRPD signals and the halo characteristic of amorphous materials (Fig. 2). Mannitol, on the other hand, was with reduced crystallinity with peaks of low intensity but good definition. In contrast to the sample freeze-dried at -10 °C, mannitol in the present sample was in δ-form according to the XRPD data (characteristic peak at 9.7° 2θ). Partial crystallization of mannitol could negatively affect the stability of the cake and cause its collapse (Johnson et al., 2002). In addition, mannitol could behave as a plasticizer (Kim et al., 1998), while the release of bound water during crystallization would negatively affect stability (Jena et al., 2016). However, no macroscopic changes or changes in physical state were observed during the three months of storage, which was confirmed by DSC and XRPD (data not shown). This could be due to the well-chosen storage temperature, which was more than 20 °C below the glass transition temperature, as recommended by Abdelwahed et al. (2006a). In the third sample with a sucrose to mannitol ratio of 3:2 (S+M 3 + 2), both excipients were in the crystalline state immediately after lyophilization (Fig. 2). However, after three months of storage, XRPD data suggested lower crystallinity of the sample, with traces of amorphous sucrose. This could be the reason for the retained stability of this sample in terms of nanocrystal particle size.

When trehalose was used as a lyoprotectant, it was amorphous in all samples, probably due to its higher Tg' (-29.8 °C) (Meng-Lund et al., 2019) (Fig. 3). Mannitol in combination with trehalose exhibited low crystallinity in both samples. Trehalose can have an effect on the crystallization of mannitol and vice versa, and the nature of this interaction is mainly determined by their ratio. In a study by Jena et al. (2016) on frozen systems, mannitol crystallized in samples with a high mannitol-trehalose ratio, while trehalose remained in the amorphous state. This was considered an ideal condition where the lyoprotectant is amorphous and thus available for interactions with the nanoparticles, while the crystalline bulking agent is providing the cake structure (Jena et al., 2016).

3.4. Morphology

Scanning electron microscopy (SEM) was used to examine the morphology of the lyophilizates. The images are shown in Figs. 4, 5, and S2. In the sample of freeze-dried dispersion without added stabilizers such as sucrose and mannitol, elongated structures and an aggregate of individual nanoparticles were visible (Fig. 4 left). Such tight clusters of nanoparticles would not allow good redispersibility. Formulations freeze-dried with primary drying at -10 °C (Fig. 4 middle and right) were highly crystalline, making it difficult to detect the nanocrystal particles. Sucrose was in the form of large, brick-like crystals, while mannitol was in the form of rod-like crystals typical of the δ-polymorph. Nanocrystal aggregates could be found on the surface of the sucrose crystals of the sample containing only sucrose (S 10%, Fig. 4 middle), and only a few aggregates were found between the mannitol crystals (S+M 3 + 2 10%, Fig. 4 right). It was obvious that nanocrystal particles interacted closely with each other, which might have led to irreversible aggregation during storage and explain the observed instability.

Similarly, nanoparticle aggregates were visible on sucrose crystals in a sample containing only sucrose and freeze-dried with primary drying at -45 °C (Figure S4, left). When sucrose and mannitol were present in equal amounts (S+M 1 + 1), both individual particles and some aggregates were visible (Figure S4, middle). This sample was more homogeneous than the previous ones, probably due to the amorphous sucrose and the very low crystallinity of the mannitol. Sample S+M 3 +

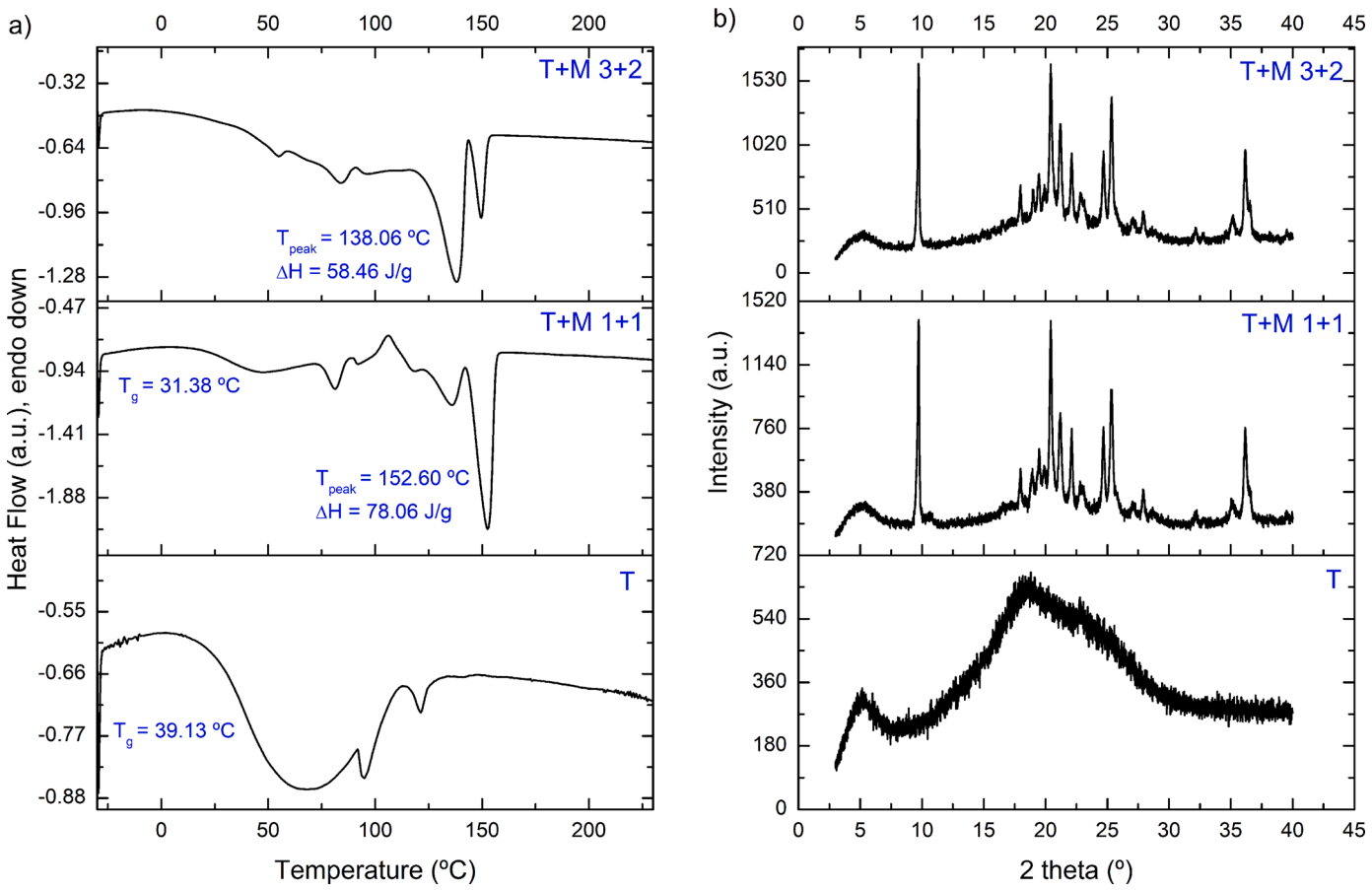

Fig. 3. DSC thermograms (a) and XRPD diffractograms (b) of freeze-dried samples with trehalose as cryo-/lyoprotectant obtained by lyophilization-2.

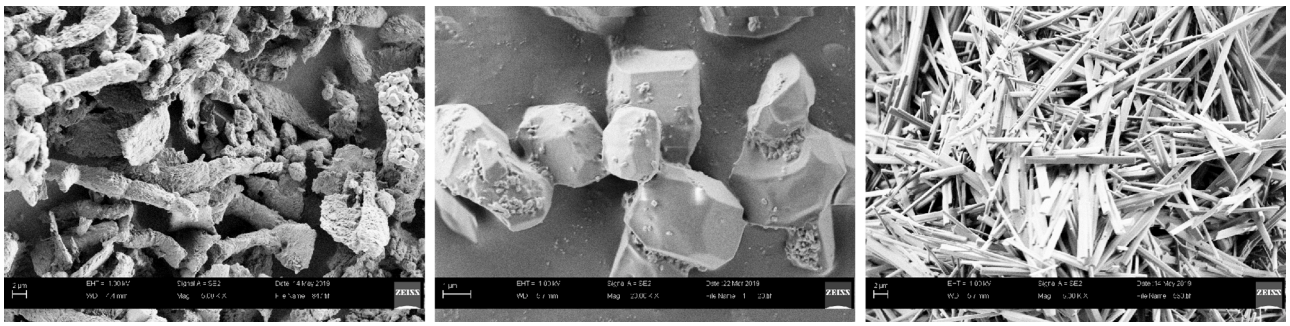

Fig. 4. Scanning electron microscopy images of freeze-dried nanocrystalline dispersions: without stabilizers, 5000 ×, scale bar 2 μm (left); with sucrose 10% (S 10%), 20,000 ×, scale bar 1 μm (middle) and with sucrose and mannitol (S+M 3 + 2 10%), 5000 ×, scale bar 2 μm (right). Lyophilization was performed with primary drying at −10 °C (lyophilization-1).

2 had a higher crystallinity, resulting in predominantly mannitol crystals visible on micrographs (Figure S4, right). These observations were particularly evident on polarized light microscopy (PLM) images. The high crystallinity of samples S and $S + M\ 3 + 2$ was again proven, while S+M 1 + 1 was almost completely amorphous. Several crystalline parts of the sample probably consisted of mannitol and nanocrystals (Fig. S5).

Samples containing trehalose as a lyoprotectant differed from those containing sucrose. Due to the amorphous state of trehalose and the low crystallinity of mannitol, all samples had a very homogeneous matrix, as visible on SEM and PLM images (Figs. 5 and S5). This was explicitly evident on a microscopic image of sample T+M 1 + 1, where individual nanoparticles are embedded in the matrix (Fig. 5, center). The amorphous matrix was confirmed in PLM images, in which the nanoparticles were also detected as crystalline clusters distributed throughout the samples (Figure S5). All observations were consistent with the results of solid state analysis by DSC and XRPD.

3.5. Fourier transform infrared (FT-IR) spectroscopy

According to the water replacement hypothesis, hydrogen bonds between lyoprotectants and nanocrystalline stabilizers are required to obtain nonaggregated lyophilizates (Trenkenschuh and Friess, 2021). One of the valuable techniques to study these interactions is Fourier transform infrared spectroscopy (FT-IR) (Kumar et al., 2014). Information about hydrogen bonding can be inferred from analysis of the position and width of the OH-stretching band in the FT-IR spectrum (Sritham and Gunasekaran, 2017). In this study, the analysis included the interpretation of the transmission spectra of bulk excipients (sucrose,

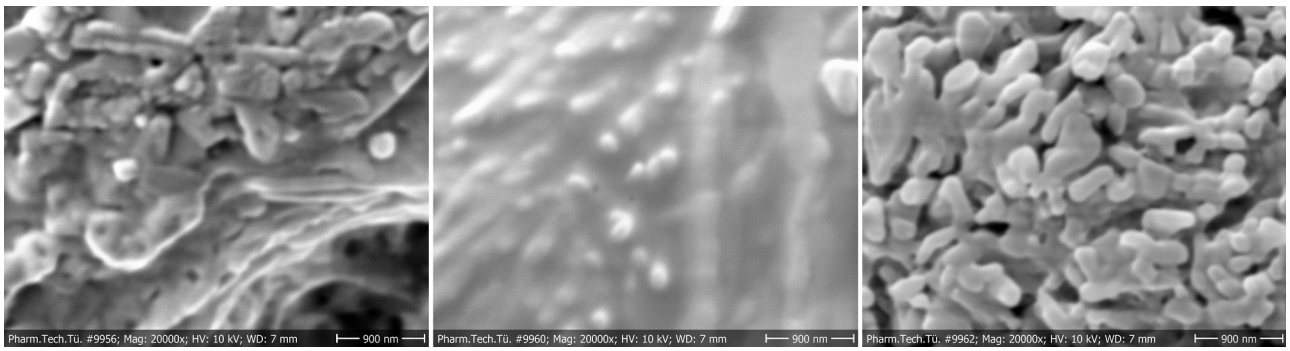

Fig. 5. Scanning electron microscopy images of freeze-dried nanocrystalline dispersions: with trehalose (T) (left); with trehalose and mannitol T+M 1 + 1 (middle) and with trehalose and mannitol T+M 3 + 2 (right). The magnification was 20,000 ×, scale bar 900 nm in all images. Lyophilization was performed with primary drying at -45 °C (lyophilization-2).

trehalose, and mannitol) and six lyophilizates obtained by freeze-drying with primary drying at -45 °C (S, S+M 1 + 1, S+M 3 + 2, T,T+M 1 + 1, and T+M 3 + 2). FT-IR Spectra are shown in Figs. 6 and 7. Although FT-IR analysis revealed numerous well-defined transmission bands in DK-I-56-1 (data not shown), they could not be singled out in any lyophilizate spectra due to the low concentration of this compound. For the same reason, the nanocrystal stabilizers (polysorbate 80 and poloxamer 407) were not visible.

FT-IR spectra of bulk sucrose, trehalose, and mannitol were in accordance to the findings in the related literature (Brizuela et al., 2012; Wolkers et al., 2004; Bruni et al., 2009). The transmission spectrum of sucrose was characterized by very sharp and well-defined bands. The OH-stretching band was located at 3316 cm^{-1}, which is typical for carbohydrates, while the isolated peak at around 3500 cm^{-1} was assumed to be related to the weak hydrogen bonding between sugar molecules. Five bands in the CH-stretching region were located around 2941 cm^{-1}. The fingerprint region between 1500 and 800 cm^{-1} consisted of distinct and partially overlapping bands originating from CO-stretching, CC-stretching, and COH-bending vibrations (Sritham and Gunasekaran, 2017).

In lyophilizate S, which contained only sucrose as a lyoprotectant, the position of the OH-stretching band was shifted to a lower wavelength number. In the other two samples, S+M 1 + 1 and S+M 3 + 2, the shift was even more pronounced, and signals were with the increased intensity (Fig. 6b). The changed position of the band was associated with the changed environment of the mentioned functional group. The decrease in the average length of the hydrogen bonds in the sugar matrix leads to a decrease in the wavenumber of the OH-stretching band (Wolkers et al., 2004). The hydroxyl group involved in hydrogen bonding would have a lower binding force constant due to the delocalization of electrons in hydrogen bonded structures (Ottenhof et al., 2003). Therefore, the magnitude of the band shift could be related to the strength of the hydrogen bonds. It was found that the interaction was more pronounced when mannitol was added, and when comparing two samples with the combination of sucrose and mannitol, a higher sucrose to mannitol ratio favored hydrogen bonding. This suggests that the interactions were promoted in the presence of mannitol, while sucrose was mainly responsible for stabilization. Although the presence of water can also lead to a shift in the wavenumber of the OH-stretching band (Sritham and Gunasekaran, 2017), the moisture content was similar in all samples (about 3%), so its influence could be excluded when comparing different freeze-dried samples.

The FT-IR spectrum of trehalose dihydrate *in bulk* was typical for crystalline substances, with the same spectral regions as sucrose. The sharp and intense peaks came from the higher degree of homogeneity of the intermolecular interactions, resulting in fewer dispersed vibrational levels. However, much broader transmission bands were visible in the samples containing amorphous trehalose (lyophilizates T, T+M 1 + 1 and T+M 3 + 2). The band width is associated with the distribution of the length and orientation of the bonds formed (Sritham and

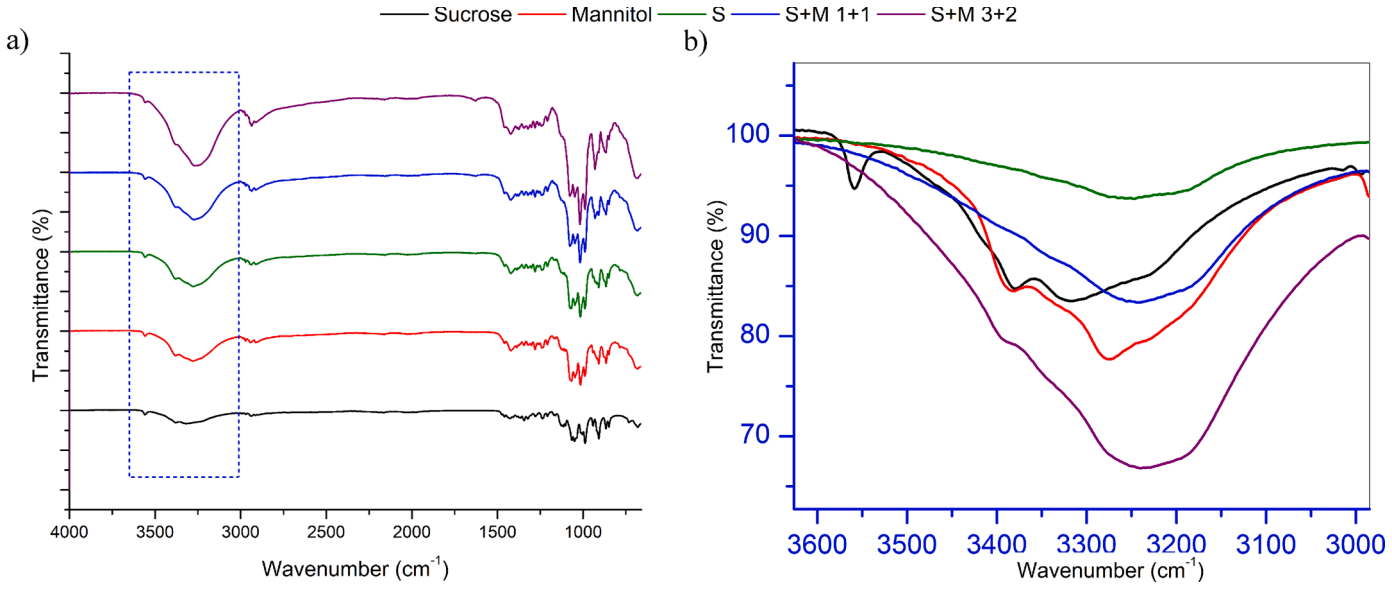

Fig. 6. FT-IR spectra of freeze-dried samples with sucrose as lyoprotectant: from 4000 to 660 cm^{-1} (a) and selected area from 3600 to 3000 cm^{-1} (b).

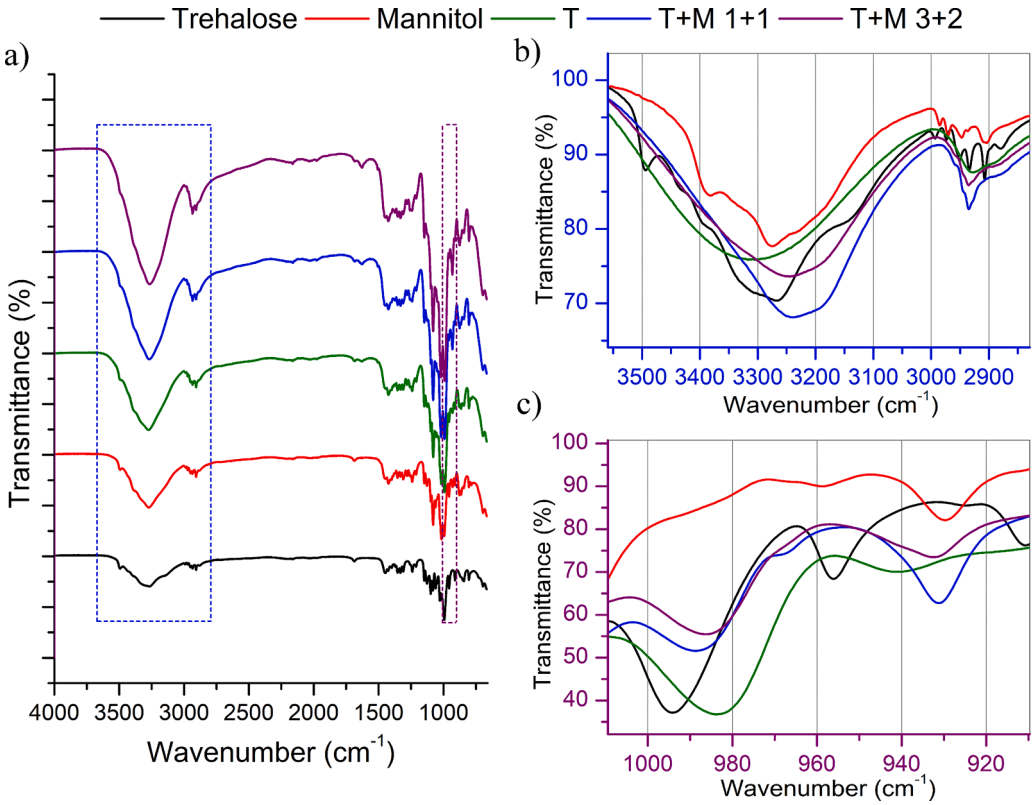

Fig. 7. FT-IR spectra of freeze-dried samples with trehalose as lyoprotectant: from 4000 to 660 cm^{-1} (a) and selected areas from 3600 to 3000 cm^{-1} (b) and from 1000 to 920 cm^{-1} (c).

Gunasekaran, 2017). The band at 3500 cm^{-1} in the untreated trehalose, corresponding to the stretch vibration of the two crystal water molecules in the dihydrate, disappeared in the spectra of the freeze-dried samples, similarly as in Jakubowska et al. (2022) (Fig. 7b). In addition, the peak associated with the crystal water in the trehalose dihydrate at 1680 cm^{-1} shifted to 1640 cm^{-1} in the freeze-dried samples (Fig. 7a). These observations clearly indicated the presence of amorphous material with water adsorbed on its surface (Akao et al., 2001). Additionally, six bands around 2900 cm^{-1} (CH-stretching region) from the crystalline trehalose (the bulk material) were replaced by a broad peak in lyophilzate T, similarly as in Wolkers et al. (2004).

As for the OH-stretching band, the position of the this band shifted from 3268 to 3316 cm^{-1} in the sample with trehalose alone (sample T) in contrast to the S sample, where a shift to lower wavenumbers occurred, indicating an increase in hydrogen bond lengths and a wide range of their orientations (Sritham and Gunasekaran, 2017; Wolkers et al., 2004). In contrast, a downward shift of this band was observed in samples T+M 1 + 1 and T+M 3 + 2 (Fig. 7b). Since it was not as pronounced as in the samples with sucrose, this result suggests a lower degree of interaction with the nanocrystals.

Two peaks visible in the spectrum of the untreated trehalose at 994 and 956 cm^{-1} could correspond to the vibrational modes (antisymmetric and symmetric stretching) of the glycoside bond. In different trehalose forms, these bands could be shifted, indicating different conformations about the glycoside linkage. The sugar molecules could be in different conformational states in which the hydroxyl groups of trehalose could form hydrogen bonds with water (Akao et al., 2001). In sample T, the bands at 984 and 941 m^{-1} could indicate an open structure of the trehalose molecule, but unable to form a significant number of hydrogen bonds. For the other two samples (T+M 1 + 1 and T + M 3 + 2), the position of the bands at 989 and 931 cm^{-1} and 986 and 932 cm^{-1} for the first and second sample, respectively, indicates a more closed conformation (Fig. 7c). It was demonstrated that the greater affinity for water could reduce the molecular mobility of the vitreous matrix and contribute to the stability during storage. However, under conditions with high residual water content, crystallization of trehalose could be induced On the other hand, the resulting lower affinity of trehalose for water could be advantageous for the long-term storage in samles with high moisture content (Starciuc et al., 2020). This could explain the excellent stability of the lyophilizates with almost unchanged RDI despite the high residual water (ca. 3.4%), which could not be lowered in spite the prolonged secondary drying.

4. Conclusion

Nanocrystal dispersions of DK-I-56-1 were successfully freeze-dried with different combinations of lyoprotectant and bulking agent. Although the particle size remained almost unchanged during the different lyophilization processes, proper selection of excipients as well as process parameters was crucial for improving stability during storage. While a sufficient amount of lyoprotectant is required to stabilize the nanocrystals in the dried state, the bulking agent in the right concentration is necessary to maintain the cake structure. For freeze-dried samples that were primarily dried at -10 °C, the changes that occurred during storage affected the stability despite the good redispersibility immediately after lyophilization. According to the results of this study, primary drying should be performed below Tg' to promote interactions between lyoprotectant and the nanocrystals. In all cases, a sucrose/trehalose to mannitol ratio of 3:2 at a total concentration of 10% lead to the maintenance of particle size during lyophilization and three months of storage, with particle size remaining in the submicron range. Sucrose was superior to trehalose in maintaining particle size during freeze-drying, probably due to its greater interactions with nanocrystals. On the other hand, trehalose was more effective in maintaining unchanged particle size during three months of storage irrespective of the formulation composition. The reason for this could be found in the

homogeneous matrix formed in samples with trehalose and the lower affinity of the formed conformation of amorphous trehalose for water. However, stronger intermolecular interactions in formulation with optimal sucrose to mannitol ratio provided redispersibility index of around 95% after three months of storage, emphasizing their essential role in nanocrystal stability.

CRediT authorship contribution statement

Jelena R. Mitrović: Conceptualization, Methodology, Investigation, Writing – original draft. **Maja Bjelošević Žiberna:** Methodology, Writing – original draft. **Aleksandar Vukadinović:** Investigation, Writing – review & editing. **Daniel E. Knutson:** Investigation, Writing – review & editing. **Dishary Sharmin:** Writing – review & editing. **Aleksandar Kremenović:** Writing – review & editing. **Pegi Ahlin Grabnar:** Writing – review & editing. **Odon Planinšek:** Investigation. **Dominique Lunter:** Investigation. **James M. Cook:** Writing – review & editing, Supervision, Funding acquisition. **Miroslav M. Savić:** Conceptualization, Writing – review & editing, Supervision, Funding acquisition. **Snežana D. Savić:** Conceptualization, Writing – review & editing, Supervision, Funding acquisition.

Data availability

No data was used for the research described in the article.

Acknowledgment

This research was supported by the Science Fund of the Republic of Serbia, through grant No. 7749108, the project *Neuroimmune aspects of mood, anxiety and cognitive effects of leads/drug candidates acting at GABAA and/or sigma-2 receptors: In vitro/in vivo delineation by nano- and hiPSC-based platforms-NanoCellEmoCog*. We would also like to acknowledge the National Institutes of Health, USA (R01 NS076517, R01 MH096463 to JC) and National Science Foundation, Division of Chemistry (CHE- 1625735 to JC). The authors would also like to thank Mr. Klaus Weyhing, Department of Pharmaceutical Technology at University of Tübingen and dr Vladimir Dobričić, Department of Pharmaceutical Chemistry, University of Belgrade – Faculty of Pharmacy for their experimental assistance.

Supplementary materials

Supplementary material associated with this article can be found, in the online version, at doi:10.1016/j.ejps.2023.106557.

References

Abdelwahed, W., Degobert, G., Stainmesse, S., Fessi, H., 2006a. Freeze-drying of nanoparticles: formulation, process and storage considerations. Adv. Drug Deliv. Rev. 58 (15), 1688–1713. https://doi.org/10.1016/j.addr.2006.09.017.

Akao, K.I., Okubo, Y., Asakawa, N., Inoue, Y., Sakurai, M., 2001. Infrared spectroscopic study on the properties of the anhydrous form II of trehalose. Implications for the functional mechanism of trehalose as a biostabilizer. Carbohydr. Res. 334 (3), 233–241. https://doi.org/10.1016/s0008-6215(01)00182-3.

Al-Kassas, R., Bansal, M., Shaw, J., 2017. Nanosizing techniques for improving bioavailability of drugs. J Control Release 260, 202–212. https://doi.org/10.1016/j.jconrel.2017.06.003.

Anko, M., Bjelošević, M., Planinšek, O., Trstenjak, U., Logar, M., Grabnar, P.A., Brus, B., 2019. The formation and effect of mannitol hemihydrate on the stability of monoclonal antibody in the lyophilized state. Int. J. Pharm. 564, 106–116. https://doi.org/10.1016/j.ijpharm.2019.04.044.

Abdelwahed, W., Degobert, G., Fessi, H., 2006b. Investigation of nanocapsules stabilization by amorphous excipients during freeze-drying and storage. Eur. J. Pharm. Biopharm. 63 (2), 87–94. https://doi.org/10.1016/j.ejpb.2006.01.015.

Beirowski, J., Inghelbrecht, S., Arien, A., Gieseler, H., 2011. Freeze drying of nanosuspensions, 2: the role of the critical formulation temperature on stability of drug nanosuspensions and its practical implication on process design. J. Pharm. Sci. 100 (10), 4471–4481. https://doi.org/10.1002/jps.22634.

Bjelošević, M., Pobirk, A.Z., Planinšek, O., Grabnar, P.A., 2020. Excipients in freeze-dried biopharmaceuticals: contributions toward formulation stability and lyophilisation cycle optimisation. Int. J. Pharm. 576, 119029 https://doi.org/10.1016/j.ijpharm.2020.119029.

Brizuela, A.B., Bichara, L.C., Romano, E., Yurquina, A., Locatelli, S., Brandán, S.A., 2012. A complete characterization of the vibrational spectra of sucrose. Carbohydr. Res. 361, 212–218. https://doi.org/10.1016/j.carres.2012.07.009.

Bruni, G., Berbenni, V., Milanese, C., Girella, A., Cofrancesco, P., Bellazzi, G., Marini, A., 2009. Physico-chemical characterization of anhydrous D-mannitol. J. Therm. Anal. Calorim. 95 (3), 871–876. https://doi.org/10.1007/s10973-008-9384-5.

Divović Matović, B., Knutson, D., Mitrović, J., Stevanović, V., Stanojević, B., Savić, S., Cook, J.M., Savić, M.M., 2022. Behavioural interaction of pyrazoloquinolinone positive allosteric modulators at α6GABAA receptors and diazepam in rats: anti-diazepam-induced ataxia action as a structure-dependent feature. Basic Clin. Pharmacol. Toxicol. 131 (6), 514–524. https://doi.org/10.1111/bcpt.13801.

Gol, D., Thakkar, S., Misra, M., 2018. Nanocrystal-based drug delivery system of risperidone: lyophilization and characterization. Drug Dev. Ind. Pharm. 44 (9), 1458–1466. https://doi.org/10.1080/03639045.2018.1460377.

Holzer, M., Vogel, V., Mäntele, W., Schwartz, D., Haase, W., Langer, K., 2009. Physico-chemical characterisation of PLGA nanoparticles after freeze-drying and storage. Eur. J. Pharm. Biopharm. 72 (2), 428–437. https://doi.org/10.1016/j.ejpb.2009.02.002.

Jakubowska, E., Bielejewski, M., Milanowski, B., Lulek, J., 2022. Freeze-drying of drug nanosuspension–study of formulation and processing factors for the optimization and characterization of redispersible cilostazol nanocrystals. J. Drug Deliv. Sci. Technol. 74, 103528 https://doi.org/10.1016/j.jddst.2022.103528.

Jena, S., Suryanarayanan, R., Aksan, A., 2016. Mutual influence of mannitol and trehalose on crystallization behavior in frozen solutions. Pharm. Res. 33, 1413–1425. https://doi.org/10.1007/s11095-016-1883-7.

Johnson, R.E., Kirchhoff, C.F., Gaud, H.T., 2002. Mannitol–sucrose mixtures—versatile formulations for protein lyophilization. J. Pharm. Sci. 91 (4), 914–922. https://doi.org/10.1002/jps.10094.

Kim, A.I., Akers, M.J., Nail, S.L., 1998. The physical state of mannitol after freeze-drying: effects of mannitol concentration, freezing rate, and a noncrystallizing cosolute. J. Pharm. Sci. 87 (8), 931–935. https://doi.org/10.1021/js980001d.

Knutson, D.E., Kodali, R., Divović, B., Treven, M., Stephen, M.R., Zahn, N.M., Dobričić, V., Huber, A.T., Meirelles, M.A., Verma, R.S., et al., 2018. Design and synthesis of novel deuterated ligands functionally selective for the γ-aminobutyric acid type a receptor (GABAAR) α6 subtype with improved metabolic stability and enhanced bioavailability. J. Med. Chem. 61 (6), 2422–2446. https://doi.org/10.1021/acs.jmedchem.7b01664.

Kumar, S., Gokhale, R., Burgess, D.J., 2014. Sugars as bulking agents to prevent nanocrystal aggregation during spray or freeze-drying. Int. J. Pharm. 471 (1–2), 303–311. https://doi.org/10.1016/j.ijpharm.2014.05.060.

L Remmele, R., Krishnan, S., J Callahan, W., 2012. Development of stable lyophilized protein drug products. Curr. Pharm. Biotechnol. 13 (3), 471–496. https://doi.org/10.2174/138920112799361990.

Li, J., Wang, Z., Zhang, H., Gao, J., Zheng, A., 2021. Progress in the development of stabilization strategies for nanocrystal preparations. Drug Deliv. 28, 19–36. https://doi.org/10.1080/10717544.2020.1856224.

Liao, X., Krishnamurthy, R., Suryanarayanan, R., 2007. Influence of processing conditions on the physical state of mannitol—implications in freeze-drying. Pharm. Res. 24 (2), 370–376. https://doi.org/10.1007/s11095-006-9158-3.

Meng-Lund, H., Holm, T.P., Poso, A., Jorgensen, L., Rantanen, J., Grohganz, H., 2019. Exploring the chemical space for freeze-drying excipients. Int. J. Pharm. 566, 254–263. https://doi.org/10.1016/j.ijpharm.2019.05.065.

Mitrović, J.R., Divović, B., Knutson, D.E., Đoković, J.B., Vulić, P.J., Randjelović, D.V., Dobričić, V.D., Čalija, B.R., Cook, J.M., Savić, M.M., Savić, S.D., 2020. Nanocrystal dispersion of DK-I-56-1, a poorly soluble pyrazoloquinolinone positive modulator of α6 GABAA receptors: formulation approach toward improved *in vivo* performance. Eur. J. Pharm. Sci. 152, 105432 https://doi.org/10.1016/j.ejps.2020.105432.

Mohammady, M., Yousefi, G., 2020. Freeze-drying of pharmaceutical and nutraceutical nanoparticles: the effects of formulation and technique parameters on nanoparticles characteristics. J. Pharm. Sci. 109 (11), 3235–3247. https://doi.org/10.1016/j.xphs.2020.07.015.

Niu, L., Panyam, J., 2017. Freeze concentration-induced PLGA and polystyrene nanoparticle aggregation: imaging and rational design of lyoprotection. J. Control. Release 248, 125–132. https://doi.org/10.1016/j.jconrel.2017.01.019.

Ottenhof, M.A., MacNaughtan, W., Farhat, I.A., 2003. FTIR study of state and phase transitions of low moisture sucrose and lactose. Carbohydr. Res. 338 (21), 2195–2202. https://doi.org/10.1016/s0008-6215(03)00342-2.

Patel, D., Zode, S.S., Bansal, A.K., 2020. Formulation aspects of intravenous nanosuspensions. Int. J. Pharm. 586, 119555 https://doi.org/10.1016/j.ijpharm.2020.119555.

Patel, S.M., Nail, S.L., Pikal, M.J., Geidobler, R., Winter, G., Hawe, A., Davagnino, J., Gupta, S.R., 2017. Lyophilized drug product cake appearance: what is acceptable? J. Pharm. Sci. 106 (7), 1706–1721. https://doi.org/10.1016/j.xphs.2017.03.014.

Sieghart, W., Chiou, L.C., Ernst, M., Fabjan, J., Savić, M.M., Lee, M.T., 2022. α6-Containing GABAA receptors: functional roles and therapeutic potentials. Pharmacol. Rev. 74 (1), 238–270. https://doi.org/10.1124/pharmrev.121.000293.

Sritham, E., Gunasekaran, S., 2017. FTIR spectroscopic evaluation of sucrose-maltodextrin-sodium citrate bioglass. Food Hydrocoll. 70, 371–382. https://doi.org/10.1016/j.foodhyd.2017.04.023.

Starciuc, T., Malfait, B., Danede, F., Paccou, L., Guinet, Y., Correia, N.T., Hedoux, A., 2020. Trehalose or sucrose: which of the two should be used for stabilizing proteins in the solid state? A dilemma investigated by in situ micro-raman and dielectric relaxation spectroscopies during and after freeze-drying. J. Pharm. Sci. 109 (1), 496–504. https://doi.org/10.1016/j.xphs.2019.10.055.

Trenkenschuh, E., Friess, W., 2021. Freeze-drying of nanoparticles: how to overcome colloidal instability by formulation and process optimization. Eur. J. Pharm. Biopharm. 165, 345–360. https://doi.org/10.1016/j.ejpb.2021.05.024.

Trenkenschuh, E., Savšek, U., Friess, W., 2021. Formulation, process, and storage strategies for lyophilizates of lipophilic nanoparticulate systems established based on the two models paliperidone palmitate and solid lipid nanoparticles. Int. J. Pharm. 606, 120929 https://doi.org/10.1016/j.ijpharm.2021.120929.

Wang, W., 2015. Tolerability of hypertonic injectables. Int. J. Pharm. 490 (1–2), 308–315. https://doi.org/10.1016/j.ijpharm.2015.05.069.

Wolkers, W.F., Oliver, A.E., Tablin, F., Crowe, J.H., 2004. A Fourier-transform infrared spectroscopy study of sugar glasses. Carbohydr. Res. 339 (6), 1077–1085. https://doi.org/10.1016/j.carres.2004.01.016.

Wu, L., Zhang, J., Watanabe, W., 2011. Physical and chemical stability of drug nanoparticles. Adv. Drug Deliv. Rev. 63 (6), 456–469. https://doi.org/10.1016/j.addr.2011.02.001.

Yue, P., Xiao, M., Xie, Y., Ma, Y., Guan, Y., Wu, Z., Hu, P., Wang, Y., 2016. The roles of vitrification of stabilizers/matrix formers for the redispersibility of drug nanocrystals after solidification: a case study. AAPS PharmSciTech 17, 1274–1284. https://doi.org/10.1208/s12249-015-0461-3.

Yue, P.F., Li, G., Dan, J.X., Wu, Z.F., Wang, C.H., Zhu, W.F., Yang, M., 2014. Study on formability of solid nanosuspensions during solidification: II novel roles of freezing stress and cryoprotectant property. Int. J. Pharm. 475 (1–2), 35–48. https://doi.org/10.1016/j.ijpharm.2014.08.041.

Yue, P.F., Li, Y., Wan, J., Yang, M., Zhu, W.F., Wang, C.H., 2013. Study on formability of solid nanosuspensions during nanodispersion and solidification: I. Novel role of stabilizer/drug property. Int. J. Pharm. 454 (1), 269–277. https://doi.org/10.1016/j.ijpharm.2013.06.050.